Analysis of Dilute Solutions of (Carboxymethyl)cellulose with the Electrostatic Wormlike Chain Theory

Richey M. Davis†

Department of Chemical Engineering, Virginia Polytechnic Institute and State University, Blacksburg, Virginia 24061

Received December 21, 1989; Revised Manuscript Received August 13, 1990

ABSTRACT: Dilute-solution data for polydisperse samples of sodium (carboxymethyl)cellulose (NaCMC) are analyzed with the electrostatic wormlike chain theory. Predictions for intrinsic viscosity $[\eta]$, translational friction favor f_0, and second virial coefficient A_2 are compared with literature data for NaCMC where the number, sedimentation, and weight averages were measured. The effects of ionic strength and molecular weight are examined. Values for $[\eta]$ and f_0 were calculated with the sedimentation–viscosity-average molecular weight, $M_{s\eta}$, while the second virial coefficient, A_2, was calculated from the number-average molecular weight, M_n, and corrected for polydispersity.

Introduction

In order to make more effective use of polyelectrolytes in applications such as colloidal stabilization[1,2] and rheology control,[3] it is necessary to understand the role played by molecular weight, backbone charge density, and solvent interactions in determining dilute-solution properties. In highly charged polyelectrolytes, electrostatic interactions dramatically change the size and conformation of the polymer molecule, giving rise to large increases in radius of gyration R_g, second virial coefficient A_2, intrinsic viscosity $[\eta]$, and the translational friction factor f_0 as the ionic strength decreases.[4] The electrostatic wormlike chain theory was developed to account for these ionic interactions for dilute solutions of monodisperse polyelectrolytes in terms of chain-stiffening and excluded-volume effects.[5-11] In a recent study, predictions from the theory were compared with light scattering and intrinsic viscosity data for nearly monodisperse potassium poly(styrenesulfonate).[10,11] Radius of gyration R_g and second virial coefficient A_2 calculations agreed with light scattering data to within 10%. Corresponding calculations for the intrinsic viscosity $[\eta]$ and translational friction factor f_0 agreed qualitatively with observed experimental trends with ionic strength and molecular weight.

In this paper, the electrostatic wormlike chain theory is tested further with light scattering, intrinsic viscosity, osmotic pressure, and sedimentation coefficient data for dilute solutions of polydisperse sodium (carboxymethyl)cellulose (NaCMC) where the number-, sedimentation–viscosity-, and weight-average molecular weights were measured. The wormlike chain theory will be reviewed in the next section.

Wormlike Chain Model. The wormlike chain theory formulated originally for nonionic polymers describes polymer chain structure in terms of the contour length L and the Kuhn length L_k, which characterizes the backbone stiffness.[12,13] The Kuhn length L_k is defined by[14a]

$$L_k = L/N_k \tag{1}$$

where N_k is the number of Kuhn segments in the molecule. Given L_k, the radius of gyration for the wormlike chain without excluded volume, R_{g0}, follows from[14b]

$$R_{g0}^2 = L^2\left\{\frac{1}{6N_k} - \frac{1}{4N_k^2} + \frac{1}{4N_k^3} - \frac{1-e^{-2N_k}}{8N_k^4}\right\} \tag{2}$$

In the limit $N_k \to \infty$, eq 2 reduces to the radius of gyration for a Gaussian coil limit and, for $N_k \to 0$, reduces to the rod limit. Thus, the wormlike chain model spans the range of conformations available to nonassociating, linear-chain polymers.

Later modifications to the model accounted for excluded-volume effects, characterized by the excluded-volume parameter z defined by[15,16]

$$z = \frac{3}{4}\left(\frac{3}{2\pi}\right)^{3/2} N_k^{1/2}\frac{\beta}{L_k^3}K(N_k) \tag{3}$$

The segmental excluded volume β is the volume around a Kuhn segment from which other segments are excluded. The function $K(N_k)$ reflects the probability of contact between any two Kuhn segments in a polymer molecule. It is obtained from the Daniels approximation to the wormlike chain segmental distribution function.[15] As a polymer molecule becomes more rodlike, the probability of segmental contacts due to random, thermal motion becomes less. Thus, as $N_k \to 0$, $K(N_k) \to 0$, indicating excluded-volume effects become less important for stiff chains.[15] In the present paper, values of $K(N_k)$ were calculated by cubic spline interpolation of tabulated values from ref 15.

The electrostatic wormlike chain theory is essentially a theory for the Kuhn length L_k and excluded volume z, which accounts for interactions between the fixed and mobile charges with the Poisson–Boltzmann equation.[5-9] Once the chain stiffness L_k and excluded-volume parameter z are determined, classical two-parameter theories are used to calculate the relevant dilute-solution properties such as the radius of gyration R_g[14c] and second virial coefficient A_2.[14d] The intrinsic viscosity $[\eta]$ and translational friction factor f_0 are calculated from the wormlike chain theory of Yamakawa and Fujii[17,18] modified to include excluded-volume effects.[10] These two-parameter theories will be discussed in more detail in later sections after a brief review of the electrostatic theory.

Electrostatic Theory. The electrostatic wormlike chain theory treats a linear polyelectrolyte in solution as a continuous cylinder with radius a, contour length L, Kuhn length L_k, and average charge spacing L_c.[5-9] Long-range intramolecular interactions generate the excluded

† This work was sponsored by the Aqualon Co., a wholly owned subsidiary of Hercules Inc.: Aqualon Co., Little Falls Centre One, 2711 Centerville Road, Wilmington, DE 19850-5417.

0024-9297/91/2224-1149$02.50/0

volume, characterized by the binary cluster integral β, while short-range interactions give rise to the chain stiffness, characterized by L_k. Unlike nonionic polymers where chain stiffness is not a strong function of solvent composition, polyelectrolytes exhibit striking increases in L_k as the ionic strength decreases due to electrostatic repulsion between the fixed charges on the backbone. The electrostatic interactions are described by the Poisson–Boltzmann equation for the dimensionless potential Ψ[19,20]

$$\nabla^2\Psi = \sinh \Psi \tag{4}$$

where Ψ is scaled on e/kT and e is the charge of an electron. The length dimension is scaled on the Debye length κ^{-1} given by

$$\kappa^{-1} = (8\pi L_b I)^{-1/2} \tag{5}$$

where I is the ionic strength. The Bjerrum length, L_b, defined by

$$L_b = e^2/4\pi\epsilon kT \tag{6}$$

is a characteristic length scale in ionic solutions.[21] In eq 6, ϵ is the solvent dielectric constant. The ratio L_b/L_c defines a dimensionless linear charge density. For low potentials, the solution of the linearized form of eq 4 with $\sinh \Psi \approx \Psi$ leads to counterion condensation where counterions are so strongly localized around a polyelectrolyte backbone that the effective dimensionless charge density is given by[21,22]

$$\begin{aligned}(L_b/L_c)_{eff} &= L_b/L_c \quad \text{for } L_b/L_c < 1\\ &= 1 \quad \text{for } L_b/L_c > 1\end{aligned} \tag{7}$$

The effective charge density is important because the excluded-volume interactions between charged segments vary as $(L_b/L_c)_{eff}^2$.[9] For highly charged polyelectrolytes such as 100% sulfonated KPSS or highly substituted NaCMC in a 1/1 salt in water at 25 °C, counterion condensation gives an effective charge density of 1 charge/0.71 nm. Counterion condensation has been successful in explaining qualitative, and, in some cases, quantitative, aspects of dilute polyelectrolyte solution behavior including effective degree of ionization, ion activity coefficients in polyelectrolyte solutions, and osmotic coefficients.[22]

A numerical solution of the nonlinear form of eq 4 for a backbone with finite diameter gives effective charge densities that differ by as much as a factor of 2 from the counterion condensation theory due to the nonlinear dependence of ion concentrations on the potential in the double layer around the backbone.[19,20] In the limit $a\kappa \to 0$, it was shown that $(L_b/L_c)_{eff}$ reached a limiting value of 0.637. Thus, excluded-volume calculations based on counterion condensation theory can be substantially in error.

The Kuhn length is the sum of nonionic effects and electrostatic interactions written as[5-8]

$$L_k = L_{k0} + L_{ke} \tag{8}$$

where L_{k0} is the bare Kuhn length reflecting the stiffness of the uncharged backbone. It is estimated from light scattering data at high ionic strengths where L_e is negligible. For Gaussian coils at the Θ-state, defined by excluded volume $z = 0$, L_{k0} is related to the radius of gyration $R_{g\theta}$ by[5]

$$L_{k0} = (6/L)R_{g\theta}^2 \tag{9}$$

The electrostatic Kuhn length L_{ke} arises due to repulsive Coulombic interactions between fixed charges on the chain. Decreasing ionic strength leads to increased Coulombic repulsion and increasing stiffness and segmental excluded volume. The expression for L_{ke} is[20]

$$L_{ke} = G^*(a\kappa, L_b/L_c)/4\kappa^2 L_b \tag{10}$$

where $G^*(a\kappa, L_b/L_c)$ is a function determined from the potential at the surface of the polyelectrolyte backbone with hard-core radius "a". Forms for the function G^* are available for two cases: (i) an analytical solution of eq 3 for the line-charge limit; i.e., $a \to 0$ and $\Psi \le 1$ so that $\sinh \Psi \approx \Psi$; and (ii) a numerical solution of eq 3 for a backbone with finite radius where the dimensionless potential Ψ can be as large as 10. For the line-charge limit and for $L_b/L_c > 1$, $G^* = 1$.[5,7,8] For case ii, the function G^* represents the correction to the line-charge theory. It is generated by a numerical solution of eq 3 and is described further in refs 10, 20, and 23. For $L_b/L_c > 1$, the line-charge theory underpredicts the electrostatic Kuhn length by more than a factor of 10 for $a\kappa > 3$. For $a\kappa \approx 10^{-1}$, the solutions from cases i and ii are similar while the line-charge theory overpredicts L_{ke} by about 20% for $a\kappa \approx 10^{-3}$.[10,20] All of the calculations of G^* in this work were made with the numerical solution for a polyelectrolyte backbone with a radius determined from atomic bond lengths.

The segmental excluded volume β is written as a sum of the effects of hard-core and electrostatic repulsion and an attractive term[9]

$$\beta = \beta_c + \beta_e + \beta_a \tag{11}$$

The hard-core contribution, β_c, is[14e]

$$\beta_c = \pi a L_k^2 \tag{12}$$

As the polymer backbone becomes more stiff, the hard-core contribution to the excluded volume increases.

The electrostatic component, β_e, was originally derived for the line-charge limit[9] in which Kuhn segments interacted with a Coulombic potential energy, V_e, so that

$$\beta_e = \int \langle 1 - \exp(-V_e)\rangle \, d\mathbf{r} \tag{13}$$

The integration in eq 13 is done over the internal coordinates in the molecule with the result

$$\beta_e = \frac{2L_k^2}{\kappa} R(w) \tag{14a}$$

with

$$w = \frac{2\pi}{L_b\kappa}\left\{\left(\frac{L_b}{L_c}\right)_{eff}\frac{1}{a\kappa K_1(a\kappa)}\right\}^2 e^{-2a\kappa} \tag{14b}$$

where $K_1(x)$ is the modified Bessel function of the second kind of order 1. Equation 14b includes modifications for the nonlinear model with finite backbone radius.[10] The calculation of the function $R(w)$ is described in ref 9 and given in the form of tabulated values and asymptotic equations. For $0.1 < w < 5.0$, tabulated values of $R(w)$ from ref 9 were used in cubic spline interpolation in the present work. For other values of w, $R(w)$ is given by the asymptotic forms

$$\begin{aligned}R(w) &= w \quad w < 0.1\\ &= (\pi/4)\{\ln w + 0.7704\} \quad w > 5.0\end{aligned} \tag{15}$$

As the ionic strength decreases, β_e increases due to increasing electrostatic repulsion between segments.

The attractive contribution to the segmental excluded volume, β_a, can be calculated by assuming a generalized van der Waals interaction between segments.[10] However, a good approximation is to treat β_a as a constant and estimate it by requiring that the total segmental excluded

volume β vanish at the Θ-state according to

$$\beta_a = -(\beta_c + \beta_e)_\Theta \quad (16)$$

Two-Parameter Thermodynamic Theories. The chain-expansion factor for the radius of gyration due to excluded-volume effects is given with reasonable accuracy by the Yamakawa–Tanaka equation[14c]

$$\alpha = \{0.541 + 0.459(1 + 6.04z)^{0.46}\}^{1/2} \quad (17)$$

The radius of gyration is a product of the chain-expansion factor due to excluded volume $\alpha(z)$ and the radius of gyration R_{g0} due solely to chain stiffening; i.e., in the absence of excluded-volume effects[5]

$$R_g = \alpha(z)\, R_{g0} \quad (18)$$

The second virial coefficient, A_2, reflects the effect of intermolecular interactions on the osmotic pressure. From the McMillan–Mayer theory of solutions, A_2 can be written as[5]

$$A_2 = (N_a N_k^2/2M^2)\beta h_0(z') \quad (19)$$

where M is the molecular weight and N_a is Avogadro's number. An approximate expression for $h_0(z')$ is[14d]

$$h_0(z') = [1 - (1 + 3.903z')^{0.4683}]/1.828z' \quad (20)$$

where

$$z' = z/[\alpha(z)]^3 \quad (21)$$

Note that the power of $\alpha(z)$ is 3 rather than $^3/_2$, which was erroneously reported in an earlier paper.[10]

For polydisperse systems, the second virial coefficient A_2* measured by osmometry is related to the second virial coefficient A_{2n} calculated with the number-average molecular weight M_n in eqs 19–21 by[14f]

$$A_2^* = q^\tau(x,\nu)\, A_{2n} \quad (22)$$

where the function $q^\tau(h,\nu)$ is given by

$$q^\tau(h,\nu) = \frac{h^\nu}{4[\Gamma(h+1)]^2}[\Gamma(h-\nu+2)\Gamma(h) + 3\Gamma(h-2\nu/3+4/3)\,\Gamma(h-\nu/3+2/3)] \quad (23)$$

where $\Gamma(x)$ is the gamma function and h is given by

$$h = [(M_w/M_n) - 1]^{-1} \quad (24)$$

For good solvents such as water/NaCl for NaCMC, the exponent $\nu = {}^1/_5$.[24]

The Schulz–Zimm molecular weight distribution was assumed in the derivation of eq 23. In terms of the z-, weight-, and number-average molecular weights, M_z, M_w, and M_n, respectively, the Schulz–Zimm distribution is given by[25a]

$$M_z{:}M_w{:}M_n = (h+2){:}(h+1){:}(h) \quad (25)$$

Monodisperse distributions occur in the limit $h \to \infty$. Decreasing values of h lead to increasing polydispersity.

Hydrodynamic Model. A hydrodynamic theory for the intrinsic viscosity $[\eta]$ and the translational friction factor f_0 must account for wormlike chain statistics to be consistent with the thermodynamic model described so far. The hydrodynamic model by Yamakawa and Fujii for intrinsic viscosity $[\eta]$[18] and the translational friction factor f_0[17] employs the Oseen tensor to account for hydrodynamic interactions between cylindrical segments of a wormlike chain with radius a. The frictional force of the solvent on the polymer chain is distributed continuously along the surface of the cylinder. Computer simulations of wormlike chain statistics in the absence of excluded volume generated expressions for $[\eta]$ and f_0 as

$$[\eta] = \frac{L^{3/2}}{M} g(N_{k'}, 2a/L_{k'}) \quad (26)$$

and

$$3\pi\eta L/f_0 = h(N_{k'}, 2a/L_{k'}) \quad (27)$$

where η is the solvent viscosity and g and h are approximate analytical expressions calculated from numerical solutions of integral equations for intramolecular hydrodynamic interactions. Due to the large number of terms in these functions, the reader is referred to refs 17, 18, and 26. In the limits $N_{k'} \to 0$ and $N_{k'} \to \infty$, eqs 26 and 27 reduce to the appropriate expressions for the intrinsic viscosity and friction factor of a rod and a Gaussian coil, respectively. Yamakawa's theory contrasts with that of Ulmann's,[27,28] whose theory for $[\eta]$ and f_0 for wormlike bead chains included one additional parameter, the friction factor per unit contour length, which Yamakawa's analysis shows to be unnecessary.

Yamakawa's theory does not include excluded-volume effects due to the difficulty of obtaining a general solution for the wormlike chain segmental distribution function for arbitrary values of z. Values of z as large as 5 are possible for highly charged polyelectrolytes such as potassium poly(styrenesulfonate).[11] Thus, the theory was adapted for polyelectrolytes by calculating the Kuhn length $L_{k'}$ an equivalent chain without excluded volume must have so that its radius of gyration equals that of a real chain having both chain stiffness and excluded volume. This renormalized Kuhn length $L_{k'}$ comes from solving the equation

$$R_{g0}(L,N_{k'}) = \alpha(z) R_{g0}(L,N_k) \quad (28)$$

for $N_{k'} = L/L_{k'}$, where N_k, R_{g0}, z, and $\alpha(z)$ are defined in eqs 1–3 and 17, respectively.[10]

This method of calculating $[\eta]$ contrasts with that of Tricot,[29,30] who assumed excluded-volume effects were negligible and fit values of $[\eta]$ to Yamakawa's theory to calculate a Kuhn length L_k and the backbone radius a. Tricot analyzed data for a variety of polyelectrolytes in water with various ionic strengths to calculate the ionic strength dependence of L_k. This method is not considered very rigorous because it ignores excluded volume and allows the backbone radius to vary with ionic strength. In the present work, however, excluded-volume effects are taken into account, albeit in an approximate manner, and the backbone radius a is kept fixed at the value determined by atomic bond lengths.

Structural Parameters for NaCMC. An important parameter in the electrostatic wormlike chain theory is the bare Kuhn length L_{k0} calculated from eq 9. This requires measurements of radius of gyration and molecular weight. Brown et al. performed light scattering, viscosity, osmometry, and sedimentation experiments on four fractions of NaCMC, designated A–D, in aqueous solutions of NaCl at 25 °C.[31-33] Brown et al. extrapolated their light scattering intensity data to zero angle to determine the weight-average molecular weight M_w and the z-average radius of gyration R_{gz} as[25b]

$$M_w = (y\text{-intercept})^{-1} \quad (29)$$

and

$$(R_{gz})^2 = \frac{3\lambda^2(\text{initial slope})}{16\pi^2 n^2(y\text{-intercept})} \quad (30)$$

where λ is the wavelength of light, n is the solvent refractive index, and (y-intercept) and (initial slope) describe the scattering curve as the scattering angle $\theta \to 0$. This extrapolation is only valid, however, with data measured at sufficiently low angles where the light scattering form factor $P(\theta)^{-1}$ lies in the range $1 < P(\theta)^{-1} \lesssim 1.3$.[25c,34-36] For Gaussian coils, $P(\theta)^{-1}$ is defined as

$$P(\theta)^{-1} = x^2/2[x - 1 + e^{-x}] \quad (31)$$

where $x = (qR_g)^2$. The scattering vector q is defined by[25c]

$$q = (4\pi n/\lambda) \sin(\theta/2) \quad (32)$$

In the low-angle limit, $P(\theta)^{-1}$ has the form

$$P(\theta)^{-1} = 1 + (qR_g)^2/3 \quad (33)$$

Brown et al. reported values for R_{gz} and the second virial coefficient A_2 from light scattering for samples A–D over a range of ionic strengths and angles so that $qR_g \gg 1$ for most cases, invalidating most of their results. However, they also measured values of R_{gz} in aqueous solutions of cadoxen (triethylenediamine cadmium hydroxide), shown in Table I, which they took to approximate the θ-conditions. Given the range of angles used, 45–135° measured in 10° increments, and the wavelength, 436 nm, the range of values of $P(\theta)^{-1}$ is shown in column 3. Data for sample D lie approximately within the acceptable range while the data for sample C lie partly outside the range. Data for samples A and B clearly fall well outside the acceptable range. Thus, only the light scattering data for sample D were used to calculate the bare Kuhn length L_{k0}. The weight-average molecular weight M_w for sample D was used to calculate the z-average molecular weight M_z from eq 25. From the values of $R_{g\theta}$ and M_z for sample D, eq 9 gives a bare Kuhn length $L_{k0} = 10.8$ nm. This differs from a reported literature value of $L_{k0} = 33.5$ nm.[37a] By contrast, the bare Kuhn length for the more flexible potassium poly(styrenesulfonate) is 2.8 nm[4] and 64 nm for the more rigid DNA.[38]

Brown et al. also measured the number-average molecular weight M_n and sedimentation–viscosity-average molecular weight $M_{s\eta}$ for samples A–D, which are listed in Table II. In addition, Brown et al. reported values for second virial coefficient A_2, intrinsic viscosity $[\eta]$, and sedimentation coefficients for NaCl concentrations ranging from 0.005 to 0.2 M. Samples B–D were made from sample A by acidic hydrolysis. The degree of carboxymethyl substitution DS was measured for all four samples at 1.06, giving an average monomer molecular weight = 247 g/mol. Thus, all samples have roughly 1 charge/monomer.

The sedimentation-average molecular weights $M_{s\eta}$ were obtained from measurements of intrinsic viscosity and sedimentation coefficient s_0 extrapolated to infinite ionic strength to suppress electrostatic effects. Values for $M_{s\eta}$ were calculated from the Flory–Mandelkern equation[39]

$$M_{s\eta} = \left[\frac{s_0[\eta]^{1/3}\eta N_a}{(\Phi^{1/3}/P)(1 - \upsilon\rho)}\right]^{3/2} \quad (34)$$

where η is the solvent viscosity, ρ is the solution density, υ is the partial specific volume of NaCMC, and N_a is Avogadro's number. The Flory–Mandelkern constant $\Phi^{1/3}/P = 2.6 \times 10^6$ for Gaussian coils, which is a reasonable assumption for high ionic strengths. For NaCMC, Brown et al. found $1 - \upsilon\rho = 0.398$.[32]

Table I
Range of Light Scattering Form Factor $P(\theta)^{-1}$ for NaCMC from Brown et al.[31]

sample	$R_{g\theta}$,[a] nm	range[b] of $P(\theta)^{-1}$	M_w,[c] kg/mol
A	82.0	1.53–4.80	
B	65.0	1.32–3.27	
C	36.5	1.10–1.63	
D	29.0	1.06–1.38	147

[a] Measured in cadoxen (triethylenediamine cadmium hydroxide); from Table VI, ref 31. [b] Calculated with eq 31 for the angular range 45–135°. [c] Weight-average molecular weight.

Table III lists the structural parameters for NaCMC. The backbone radius "a" was estimated from atomic bond lengths to be 0.5 nm. The average charge spacing $L_c = 0.49$ nm comes from assuming the charges are spread uniformly along the length of the backbone.

Attractive Binary Cluster Integral. When the Θ-state salt concentration for a polyelectrolyte at a given temperature is known, the attractive segmental excluded volume β_a can be calculated from eq 16. The Θ-state salt concentration for NaCMC at 25 °C is not known precisely. However, eq 16 still provides a useful upper bound for β_a. Figure 1 shows the calculations for β_e and β_c and their sum for NaCMC with DS = 1.06 as a function of ionic strength. As the ionic strength decreases, β_c and β_e increase monotonically with the Kuhn length L_k and the electrostatic repulsion between segments. The electrostatic segmental excluded volume β_e increases more rapidly than β_c, exceeding β_c at approximately 0.3 M. For $I = 0.01$ M, β_e exceeds β_c by 1 order of magnitude. At high ionic strengths $1.0 < I < 5.0$ M, the hard-core contribution β_c is at least 10 times greater than the electrostatic contribution β_e. For $I > 5.0$ M, the sum $\beta_e + \beta_c$ is only 5% greater than the limiting value of 187 nm^3 when $\beta_e = 0$. Thus, an ionic strength of 5.0 M was chosen as the approximate Θ-state concentration, giving the value $\beta_a \simeq -197$ nm^3.

Discussion of Results

Intrinsic Viscosity. An appropriate molecular weight average must be chosen to calculate the intrinsic viscosity $[\eta]$ and friction factor f_0 from eqs 26 and 27, respectively. The weight-average molecular weight M_w is commonly used to correlate intrinsic viscosity data according to the semiempirical Mark–Houwink equation[41]

$$[\eta] = KM^a \quad (35)$$

The sedimentation–viscosity-average molecular weight $M_{s\eta}$ is believed to be more appropriate than the weight- or number-average molecular weights since $M_{s\eta}$ is derived from intrinsic viscosity and sedimentation measurements, which probe the hydrodynamic volume of the NaCMC molecule.[40] Figure 2 shows the intrinsic viscosity data for sample D and calculations from eq 22 using the sedimentation-, number-, and weight-average molecular weights listed in Table II. Calculations with the sedimentation-average $M_{s\eta}$ clearly give the best agreement with the data, with an average overprediction of 12%. Calculations based on M_n consistently underpredict $[\eta]$ by as much as 45% and calculations based on M_w overpredict $[\eta]$ by an average of 27%. Similar results were obtained with samples A–C for comparisons between M_n and $M_{s\eta}$.

Fortelny et al. extended the Yamakawa–Fujii hydrodynamic theory to include polydispersity effects by averaging the calculations for $[\eta]$ and f_0 with the Schulz–Zimm molecular weight distribution function.[26] For chains with $N_k > 10$, their results showed that $[\eta]$ calculated from

Table II
NaCMC Characterization Data from Brown et al.[31-33]

sample	DS[a]	mol wt, kg/mol M_n[b]	$M_{s\eta}$[c]	M_w	M_z[d]	h[e]	L_{ko}/ nm
A	1.06	290	570				
B	1.06	175	440				
C	1.06	104	185				
D	1.06	70	130	147	225	0.91	10.8

[a] DS = degree of carboxymethyl substitution. Monomer molecular weight = 0.247 kg/mol. [b] Number-average molecular weight measured by osmometry. [c] Sedimentation-viscosity-average from eq 34. [d] Z-average molecular weight from eq 25. [e] Parameter in Schulz-Zimm distribution, eq 24. [f] Bare Kuhn length from eq 9.

Table III
NaCMC Structural Parameters for DS = 1.06[a]

quantity	length, nm
monomer length L_{mon}	0.52
charge spacing L_c	0.49
backbone radius a	0.50
bare Kuhn length L_{k0}	10.80

[a] Attractive segmental excluded volume $\beta_a = -197$ nm^3 at 25 °C. Dimensionless linear charge density L_b/L_c for 1-1 salt in water at 25 °C = 1.47.

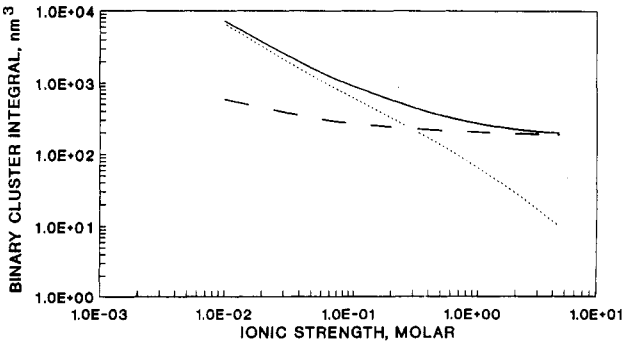

Figure 1. Ionic strength dependence of binary cluster integrals from electrostatic wormlike chain theory: (- - -) hard core; (· · ·) electrostatic; (—) hard core + electrostatic.

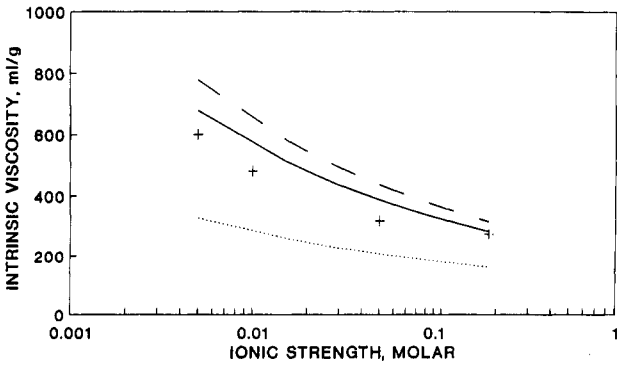

Figure 2. Effect of molecular weight average on calculations of intrinsic viscosity: (+) sample D data; (—) theory for sedimentation-viscosity-average molecular weight $M_{s\eta}$; (· · ·) theory for number-average molecular weight M_n; (- - -) theory for weight-average molecular weight M_w. Data from Brown et al.[31,32]

an average over a specified Schulz-Zimm distribution should be smaller than $[\eta]$ calculated from M_w in qualitative agreement with the present work. A detailed comparison of their calculations with the present work is not possible since their calculations lack sufficient detail.

All subsequent calculations for $[\eta]$ were made with $M_{s\eta}$ and are shown in Figure 3 along with the data. The intrinsic viscosity for sample A increases by almost 3-fold as the ionic strength decreases from 0.2 to 0.005 M, providing clear evidence of the strong electrostatic interactions that expand the polymer coil. The theory underpredicts $[\eta]$ by an average of 11% for sample A and

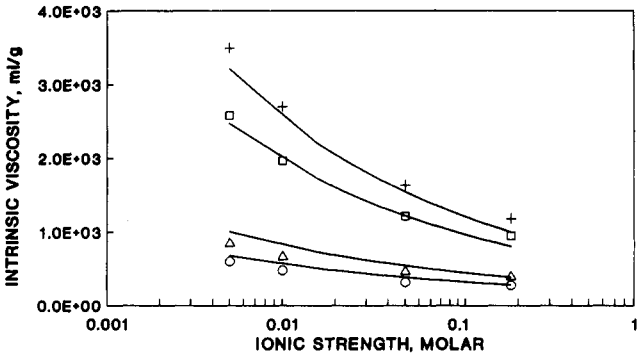

Figure 3. Intrinsic viscosity of NaCMC in NaCl at 25 °C as a function of ionic strength: (+) sample A data; (□) sample B data; (△) sample C data; (○) sample D data; (—) theory for sedimentation-viscosity-average molecular weight $M_{s\eta}$. Data from Brown et al.[31,32]

Table IV
Comparison of Kuhn Length and Backbone Diameter Calculations

I, M	L_k,[a] nm	a,[c] nm	L_k,[b] nm	a,[b] nm
0.005	46.2	0.12	24.9	0.5
0.01	36.8	0.05	19.6	0.5
0.05	22.0	0.10	14.2	0.5
0.20	16.0	0.25	12.4	0.5

[a] From Tricot.[29] [b] From electrostatic wormlike chain theory.

only 7% for sample B. For samples C and D in Figure 2, the theory overpredicts the data by an average of 13%. The agreement between experiment and theory for these NaCMC samples is significantly better than that seen for potassium poly(styrenesulfonate) where the theory overpredicted $[\eta]$ by 20-100%.[10,11]

These calculations contrast with those of Tricot, who ignored excluded-volume effects and fitted intrinsic viscosity data to Yamakawa's wormlike chain model to obtain values of L_k and backbone radius a for a variety of polymers including NaCMC from Brown et al.'s work, sodium polyacrylate, and sodium poly(styrenesulfonate).[29] In Table IV, Tricot's calculations for L_k and a for NaCMC are compared with the values of L_k calculated with eq 10 and the value $a = 0.5$ nm determined from atomic bond lengths. Tricot's values of L_k are much larger than the values calculated in the present work due to the neglect of excluded volume. At $I = 0.005$ M, the Kuhn length determined by Tricot's method is almost a factor of 2 larger than that calculated from the electrostatic wormlike chain theory. The difference between the values for L_k narrows as I increases since excluded-volume effects become less important at high ionic strengths. Tricot's calculated values for the polymer backbone radius do not vary systematically with ionic strength and, for $0.005 \leq I \leq 0.05$, are clearly not realistic. Tricot's method was also employed to calculate the persistence length for various poly(methylacrylic acid) esters in organic solvents.[30] The calculations in organic solvents may be valid due to the

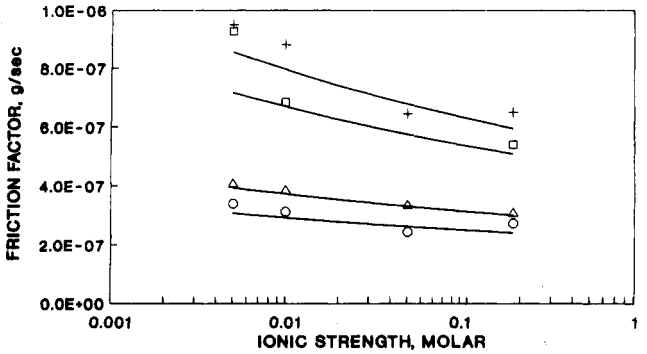

Figure 4. Translational friction factor of NaCMC in NaCl at 25 °C as a function of ionic strength: (+) sample A data; (□) sample B data; (△) sample C data; (○) sample D data; (—) theory for sedimentation–viscosity-average molecular weight $M_{s\eta}$. Data from Brown et al.[31,32]

presumed absence of electrostatic excluded-volume effects, which dominate excluded volume for polyelectrolytes in water except near the Θ-state or at high salt concentrations.

The present calculations include both chain stiffening and excluded volume in a self-consistent manner and show the relative effects of the two. For example, for sample A at I = 0.005 M, the radius of gyration calculated from eq 18 with the sedimentation-average molecular weight $M_{s\eta}$ is 99 nm. The radius of gyration in the absence of excluded volume, R_{g0}, calculated from eq 2 is 69 nm, and the chain expansion factor due to excluded-volume effects, $\alpha(z)$, from eq 17 is 1.43.

Translational Friction Factor. To be consistent with the modified Yamakawa theory for $[\eta]$, it is necessary to use $M_{s\eta}$ to calculate f_0 from eq 27. The translational friction factor f_0 was calculated from the sedimentation coefficient s and the sedimentation–viscosity-average molecular weight $M_{s\eta}$ from[38b]

$$f_0 = M_{s\eta}(1 - v\rho)/N_a s \tag{36}$$

The calculations for all four samples with $M_{s\eta}$ are summarized in Figure 4. In all cases, the friction factor increases as ionic strength decreases due to the increased hydrodynamic volume of the molecule. The friction factor did not change with decreasing I as dramatically as did the intrinsic viscosity. For sample A, f_0 increased by only 46% as the ionic strength decreased from 0.2 to 0.005 M. The theory for sample A agrees with the data to within an average of 8%, and two of the three data points for sample B agree with the theory to within 6%. The theory agrees with the data for sample C to within an average of 3% and, for sample D, to within an average of 8%.

Second Virial Coefficient. Given the molecular weight data for sample D in Table II, eq 22 for between the second virial coefficient derived from osmometry, A_2*, reduces to

$$A_2^* = 0.94A_{2n} \tag{37}$$

where A_{2n} is the second virial coefficient calculated from the number-average molecular weight in eq 19. For sample D at I = 0.2 M, $A_2^* = 2.46 \times 10^{-3}$ (mL·mol)/g^2 whereas the measured value from osmometry was 2.87×10^{-3} (mL·mol)/g^2, a difference of 14%. Further comparison was not possible since second virial coefficients for these samples were not reported for any lower ionic strengths. Calculations for A_2 for samples A–C were not done since values of the polydispersity parameter h from eq 24 were not available.

Conclusions

The electrostatic wormlike chain theory accounts for electrostatic interactions through the chain stiffness and excluded volume. Every parameter in this theory has a clear physical meaning and can be estimated from molecular structure or experiment. This paper outlines a general procedure for calculating the radius of gyration R_g, the intrinsic viscosity $[\eta]$, the translational friction factor f_0, and the second virial coefficient A_2* for polydisperse polyelectrolytes even for cases where the Θ-state is not known precisely. The procedure is as follows: (i) estimate the bare Kuhn length L_{k0} from light scattering data at high salt concentrations; (ii) calculate the electrostatic Kuhn length L_{ke}; (iii) estimate the attractive binary cluster integral β_a from calculations of the electrostatic and hard-core binary cluster integrals, β_e and β_c, respectively, at high ionic strength; (iv) using the appropriate molecular weight averages, calculate R_g and A_2* with standard two-parameter thermodynamic theories and $[\eta]$ and f_0 with Yamakawa's wormlike chain theory. While steps i and ii are not new to the present work, steps iii and iv involve new calculations, which allow the estimation of intrinsic viscosity and friction factor for polydisperse systems. This work also provides a revised estimate of L_{k0} for NaCMC = 10.8 nm, in contrast with a value of 33.5 nm reported earlier.

The present calculations of $[\eta]$ and f_0 are an improvement over the earlier work by Tricot, which ignored excluded-volume effects and attempted to compensate by allowing the backbone diameter to vary while fitting intrinsic viscosity data. Agreement between the data and the present model for intrinsic viscosity was typically within 14% while the agreement between data and theory for the friction factor was mostly within 8%. The present calculations also go beyond Tricot's work by calculating the translational friction factor f_0 in a manner consistent with the calculations for $[\eta]$. It was demonstrated that the sedimentation–viscosity-average molecular weight $M_{s\eta}$ is more appropriate than the weight-average molecular weight M_w in calculating $[\eta]$ and f_0.

Acknowledgment is made to the donors of the Petroleum Research Fund, administered by the American Chemical Society, for partial support of this research. I thank one of the reviewers for valuable comments on interpreting light scattering data.

References and Notes

(1) Cesarano, J., III; Aksay, I. A. *J. Am. Ceram. Soc.* **1988**, *71*, 1062.
(2) Buscall, R.; Ottewill, R. H. In *Polymer Colloids*; Buscall, R., Corner, T., Stageman, J. F., Eds.; Elsevier Applied Science Publishers: London, 1985; pp 192–211.
(3) Davis, R. M. *TAPPI J.* **1987**, *70* (No. 4), 99.
(4) Raziel, A.; Eisenberg, H. *Isr. J. Chem.* **1973**, *11*, 183.
(5) Odijk, T.; Houwaart, A. C. *J. Polym. Sci., Polym. Phys.* **1978**, *16*, 627.
(6) Odijk, T. *Polymer* **1978**, *19*, 989.
(7) Odijk, T. *J. Polym. Sci., Polym. Phys.* **1977**, *15*, 477.
(8) Skolnick, J.; Fixman, M. *Macromolecules* **1977**, *10*, 944.
(9) Fixman, M.; Skolnick, J. *Macromolecules* **1978**, *11*, 863.
(10) Davis, R. M.; Russel, W. B. *J. Polym. Sci., Polym. Phys.* **1986**, *24*, 511.
(11) Davis, R. M.; Russel, W. B. *Macromolecules* **1987**, *20*, 518.
(12) Kratky, O.; Porod, G. *Recl. Trav. Chim.* **1949**, *68*, 1106.
(13) Yamakawa, H. *Pure Appl. Chem.* **1976**, *46*, 135.
(14) Yamakawa, H. *Modern Theory of Polymer Solutions*; Harper and Row: New York, 1971; (a) p 46, (b) p 108, (c) p 163, (d) p 56, (e) p 182, (f) p 221.
(15) Yamakawa, H.; Stockmayer, W. H. *J. Chem. Phys.* **1972**, *57*, 2843.
(16) Gobush, W.; Yamakawa, H.; Stockmayer, W. H.; Magee, W. S. *J. Chem. Phys.* **1972**, *57*, 2839.

(17) Yamakawa, H.; Fujii, M. *Macromolecules* **1973**, *6*, 407.
(18) Yamakawa, H.; Fujii, M. *Macromolecules* **1974**, *7*, 128.
(19) Russel, W. B. *J. Polym. Sci., Polym. Phys.* **1982**, *20*, 1233.
(20) Fixman, M. *J. Chem. Phys.* **1982**, *76*, 6346.
(21) Manning, G. S. *J. Chem. Phys.* **1969**, *51*, 924.
(22) Manning, G. S. *Annu. Rev. Phys. Chem.* **1972**, *23*, 117.
(23) Le Bret, M. *J. Phys. (Paris)* **1981**, *292*, 291.
(24) de Gennes, P.-G. *Scaling Concepts in Polymer Physics*; Cornell University Press: Ithaca, NY, 1979; p 78.
(25) Zimm, B. H. *J. Phys. Chem.* **1948**, *16*, (a) 1099, (b) 1093, (c) 1109.
(26) Fortelny, I.; Kovar, J.; Zivny, A.; Bohdanecky, M. *J. Polym. Sci., Polym. Phys.* **1981**, *19*, 181.
(27) Ulmann, R. *J. Chem. Phys.* **1968**, *49*, 5486.
(28) Ulmann, R. *J. Chem. Phys.* **1970**, *53*, 1734.
(29) Tricot, M. *Macromolecules* **1984**, *17*, 1698.
(30) Tricot, M. *Macromolecules* **1986**, *19*, 1268.
(31) Brown, W.; Henley, D. *Makromol. Chem.* **1964**, *79*, 68.
(32) Brown, W.; Henley, D.; Ohman, J. *Arkiv. Kemi.* **1964**, *22*, 189.
(33) Brown, W.; Henley, D.; Ohman, J. *Makromol. Chem.* **1963**, *62*, 164.
(34) Holtzer, A. M.; Benoit, H.; Holtzer, A. M.; Doty, P. *J. Phys. Chem.* **1954**, *58*, 624.
(35) Benoit, H.; Holtzer, A. M.; Doty, P. *J. Phys. Chem.* **1954**, *58*, 635.
(36) Schmid, C. W., Rinehart, F. P.; Hearst, J. E. *Biopolymers* **1971**, *10*, 883.
(37) Tanford, C. *Physical Chemistry of Macromolecules*; John Wiley & Sons: New York, 1961; (a) p 497, (b) p 365.
(38) Manning, G. S. *Biopolymers* **1981**, *21*, 1751.
(39) Mandelkern, L.; Flory, P. J. *J. Chem. Phys.* **1952**, *20*, 212.
(40) Hiemenz, P. C. *Polymer Chemistry, The Basic Concepts*; Marcel Dekker: New York, 1984; p 605.
(41) Bird, R. B.; Armstrong, R. C.; Hassager, O. *Dynamics of Polymeric Liquids: Fluid Mechanics*, 2nd ed.; Wiley-Interscience, Dekker: New York, 1987; Vol. 1, p 143.

Registry No. NaCMC, 9004-32-4.